A Deployable Quasi-Yagi Monopole Antenna Using Three Origami Magic Spiral Cubes

Syed Imran Hussain Shah, *Student Member, IEEE*, Manos M. Tentzeris ⓘ, *Fellow, IEEE*, and Sungjoon Lim ⓘ, *Member, IEEE*

Abstract—We propose a deployable quasi-Yagi monopole antenna using origami magic spiral cubes, constructed from low-cost paper substrate. The proposed quasi-Yagi antenna consists of an L-shaped driven monopole, an L-shaped reflector, and two L-shaped directors. These driven monopole, reflector, and directors are designed in L-shaped geometries to achieve maximum gain in a limited cube size. The driven element and reflector are realized on the origami magic cube #1, while the two directors are designed on the magic cubes #2 and #3, respectively. The cubes are stacked together using a thin adhesive film. The presented geometry of the origami magic spiral cube antenna can be easily folded and unfolded. The dimensions in the unfolded state are 44 mm × 44 mm × 132 mm while the dimensions in the folded state are 44 mm × 44 mm × 8 mm. Therefore, in the folded state, the antenna occupies only 6% of the unfolded volume. We have numerically analyzed the antenna performance and verified the outcomes experimentally. The L-shaped reflector has increased the monopole antenna gain from 1.9 to 5.7 dBi. With the addition of two directors, the gain is further increased to 7.3 dBi at 1.9 GHz.

Index Terms—Deployable Yagi antenna, director, driven element, origami magic cube, reflector.

I. INTRODUCTION

THE Yagi antennas have several interesting features, including low cost, simple structure, ease of fabrication, high radiation efficiency, high gain, and low cross-polarization [1], [2]. These features make it a promising candidate for various modern wireless communication technologies. Previous studies have presented several Yagi antennas for various applications, but Yagi arrays operating for frequencies less than 3 GHz are somewhat bulky and have poor portability.

The origami technology offers a solution to easily transport and deploy Yagi antennas. Origami is an ancient Japanese paper folding art form, where two-dimensional (2-D) paper sheet can be creased and folded/unfolded to realize 3-D deformable and compact structures for practical applications. Various interesting origami features have been investigated previously, including tunable stiffness, multistability [3],

self-foldability [4], programmable collapse [5], and programmable curvature [6].

Thus, an origami can be used in flexible electronics [7], soft pneumatic actuators [8], self-foldable robots, foldable telescopes [9], heart stents [10], etc. The origami has also been used in architecture for a complex model design.

The origami-based techniques can be good alternatives to construct flexible, low-cost, deployable antennas as compared to the conventional antenna designs. Further, origami folding can be exploited in various antenna geometries that cannot be built using conventional methods. Compared to conventional antenna technologies, the origami approach does not require costly fabrication facilities and the manufacturing procedure is very fast. In general, a large size and space are required for a high-gain antenna and array that are not preferred in mobility. We can resolve this problem using an origami technique. For instance, the antenna size can be minimized by folding during transportation and it can be unfolded while deploying. However, only a few antennas have been proposed using such origami technology, including tetrahedron circularly polarized [11] and frequency tunable [12]–[15] antennas, where the frequency can be tuned by fully or partially unfolding the antenna. However, the geometries of these antennas were not stable against repeated folding and unfolding.

A frequency reconfigurable origami antenna has also been proposed with a foldable reflector [16]. The antenna and reflector can be folded/unfolded to adjust its size according to each desired frequency. The origami antennas can also be transformed from dipole to conical spiral antenna [17] and from a single-antenna element to series array [18]. The origami antennas can also provide polarization switching capability [19], [20]. Although a tetrahedron Yagi–Uda origami antenna has been reported in [21], the design is very large and hence, its transportation is challenging.

Therefore, we propose a deployable quasi-Yagi monopole antenna realized in an origami configuration. The driven monopole, reflector, and directors having L-shaped geometry are adopted to achieve maximum gain in the limited cube space. Dimensions in the unfolded state are 44 mm × 44 mm × 132 mm while the dimensions in the folded state are 44 mm × 44 mm × 8 mm. Therefore, in the folded state, the antenna occupies only 6% of the unfolded volume; henceforth, it can be easily transported and deployed in the unfolded state. The magic spiral cube origami is a good candidate to fold and unfold the antenna structure. Because the design is constructed from two paper sheets, the proposed antenna provides significant stability against repeated folding and unfolding, unlike the earlier reported origami
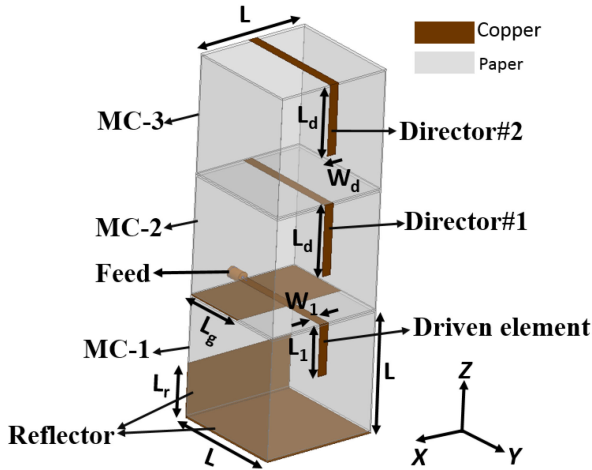
Fig. 1. Presented geometry of the origami magic spiral cube Yagi antenna in the unfolded state is $L = 44$, $L_r = 20$, $L_g = 22$, $L_1 = 20$, $L_d = 26$, and $W_1 = W_d = 3.5$ (units: millimeters).

antennas [12]–[14], [16], [17], [19]. The potential applications of the proposed antenna can be found in space and military communications.

II. ANTENNA DESIGN

Fig. 1 shows the proposed antenna geometry in the unfolded state. The antenna consists of three origami magic spiral cubes with monopole, reflector, and directors realized on the cubes. Each magic cube has been constructed from two square sheets of paper as follows.

1) Two square papers (145 × 145 mm, 0.1 mm thick) were prepared and labeled as P-I and P-II, as shown in Fig. 2(a).
2) Paper P-I was divided into the subdivisions AA′, BB′, CC′, DD′, EE′, and FF′, as shown in Fig. 2(b).
3) Segments of P-II were labeled as II′, JJ′, KK′, LL′, MM′, and NN′ as shown in Fig. 2(b).
4) P-I was folded and unfolded across AA′. AA′ acted as a border to divide paper P-I into two equilateral triangular segments, as shown in Fig. 2(c) and (d).
5) P-I was folded across FF′, as shown in Fig. 2(e), and then, folded along EE′, CC′, and BB′ as shown in Fig. 2(f)–(i). Thus, P-I now had hexagonal geometry, as shown in Fig. 2(j), comprising of two longer (BB′, EE′) and four shorter (AB, AE, A′B′, A′E′) sides.
6) P-I was separated into three segments comprising an upper pentagonal section ABG′GE, middle square section G′GHH′, and lower pentagonal section H′B′A′E′H, as shown in Fig. 2(k).
7) A copper film (44 × 22 × 0.1 mm; length, width, and thickness, respectively) was pasted on a subportion of the middle square section G′GHH′, as shown in Fig. 2(k).
8) The lower pentagonal section H′B′A′E′H [see Fig. 2(k)] was folded in the direction of the middle square segment G′GHH′ [see Fig. 2(k)], converting the hexagonal paper to pentagonal geometry.
9) Section G′A′H was folded in the direction of G′H′H [see Fig. 2(l)], and section G′BAEG was folded downward [see Fig. 2(m) and (n)].

10) Section G′BAE was folded in the direction of G′GE to obtain a hexagonal geometry [see Fig. 2(o)].
11) Sheet P-II was folded exactly as P-I to create another hexagonal shaped folded geometry, as shown in Fig. 2(p). The magic cube was created by joining the folded geometries formed from P-I and P-II (see Fig. 2(o) and (p), respectively).

Fig. 2(q) shows that the magic cube has six square sides; each of them has the same dimensions. The magic cube geometry can be conveniently folded and unfolded [see Fig. 2(r)]. After fabricating the magic cube, the monopole driven element is realized on magic cube #1 (MC-1), using copper film [see Fig. 2(s)].

The copper film, because of its flexible and resilient to crack properties, has been appropriately used in origami-based antenna applications, which goes through several folding and unfolding cycles. The magic cubes #2 and #3 (MC-2 and MC-3) are also fabricated using the same procedure as for MC-1, where the copper film realizes the monopole antenna directors, [see Fig. 2(t) and (u)]. The proposed prototype antenna was completed after joining all three magic cubes using a double-sided bonding film. Fig. 2(v) and (w) shows the spiral magic cube antenna geometry in its unfolded and folded states, respectively. A folded state antenna volume is only 6% of that in the unfolded state. This smaller folded state is very suitable for transportation. The antenna can be easily transported in the folded state and conveniently deployed in the unfolded state.

The proposed antenna structure was designed and simulated using the ANSYS high-frequency structure simulator. A plain paper substrate was modeled with relative permittivity and dielectric loss tangent of 2.2 and 0.06, respectively. The conductivity of the copper foil is 0.44 MS/m [12], which is lower than the nominal conductivity of the copper because of the adhesive material. Due to lower conductivity, the radiation efficiency is decreased from 74% to 64%.

For accurate analysis, a subminiature version A connector was included in the electromagnetic simulation. The L-shaped antenna was designed for MC-1 to resonate at 1.9 GHz without any reflector or director. Then, the L-shaped reflector was added to MC-1 to increase the antenna peak gain. Two L-shaped directors were, then, added to MC-2 and MC-3, respectively, to further increase the antenna gain. Fig. 3(a) shows the parametric study for the L-shaped driven monopole short arm length (L_1). Resonance frequencies are obtained at 2.08, 2.01, 1.9, 1.85, and 1.78 GHz corresponding to $L_1 = 16$, 18, 20, 22, and 24 mm, respectively. Thus, increasing L_1 decreases the resonance frequency, and $L_1 = 20$ mm is chosen to obtain the desired resonance frequency (1.9 GHz). Fig. 3(b) shows the reflection coefficients for different driven monopole element width (W_1). Impedance matching was improved by increasing W_1 to 3.5 mm. The further increase of W_1 deteriorates impedance matching. Thus, we selected $W_1 = 3.5$ mm rather than 2.5 mm considering the fabrication difficulty. Next, the L-shaped directors are designed to maximize the peak gain.

In Fig. 3(c), directivity and radiation efficiency of the antenna are plotted for different short arm lengths (L_d) of the directors. As the short arm length increases up to $L_d = 26$ mm, the directivity of the antenna is increased while the radiation efficiency is decreased.

In Fig. 3(d), directivity and radiation efficiency of the antenna are plotted for different widths (W_d) of the directors. It
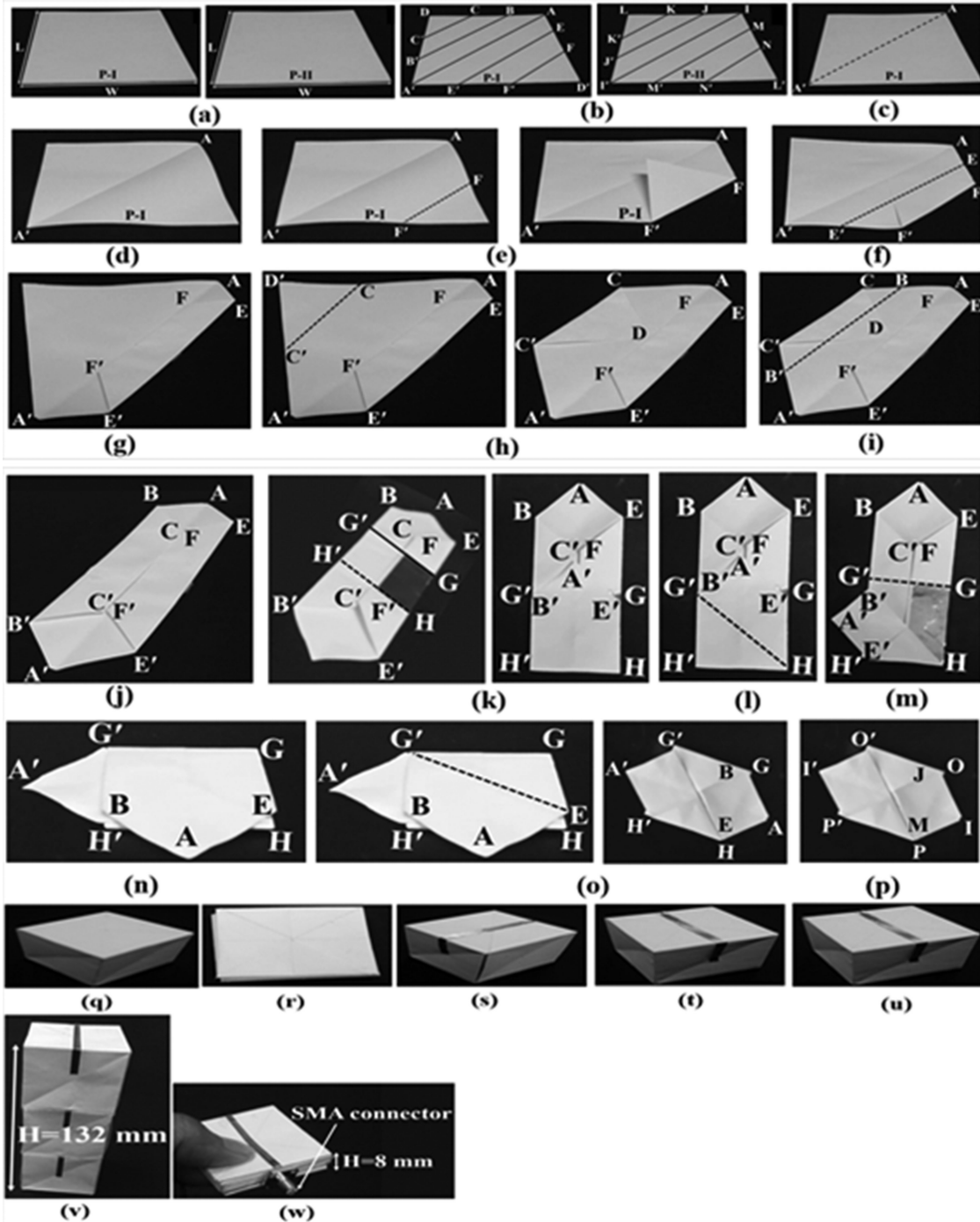
Fig. 2. Fabrication steps for the proposed antenna. (a) Paper sheet P-I and P-II. (b) P-I and P-II marked with subdivisions. (c), (d) Folding-unfolding P-I across AA′. (e) Folding across FF′. (f), (g) Folding across EE′. (h) Folding across CC′. (i) Folding across BB′. (j) Hexagonal formed paper. (k) Folding across HH′. (l) Folding across G′H. (m), (n) Folding across GG′. (o) Folding across EG′. (p) Folded geometry of P-II. (q) Magic cube. (r) Magic cube in folded form. (s) MC-1 with attached monopole. (t) MC-2 with attached director. (u) MC-3 with attached director. (v) Antenna in unfolded form. (w) Antenna in folded form.

is observed that both directivity and radiation efficiency are increased until W_d reaches 3.5 mm. Therefore, in order to design the antenna with highest directivity and reasonable radiation efficiency, $L_d = 26$ mm and $W_d = 3.5$ mm for the directors are selected, where the directivity and radiation efficiency are 10.23 dB and 64%, respectively.

Fig. 4 shows the simulated 3-D radiation patterns at 1.9 GHz. The simple monopole antenna without the reflector and director

[see Fig. 4(a)] exhibits an omnidirectional radiation with 1.9 dBi peak gain. Loading the L-shaped reflector [see Fig. 4(b)], the antenna emits a broadside radiation with 5.7 dBi peak gain. Loading of one L-shaped director is shown in Fig. 4(c). The L-shaped monopole antenna, with the reflector and one director, achieves 6.8 dBi peak gain, while the peak gain is enhanced to 8.3 dBi with reflector and two directors [see Fig. 4(d)]. In this work, we decide to load two directors in order to maximize
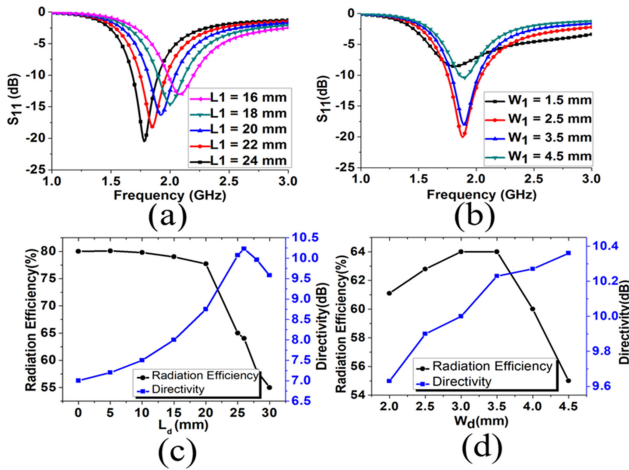
Fig. 3. Parametric study of S11 for (a) different driven monopole short arm length (L_1) and (b) driven monopole width (W_1). The parametric study of directivity and radiation efficiency for (c) different director short arm length (L_d) and (d) different director widths (W_d).
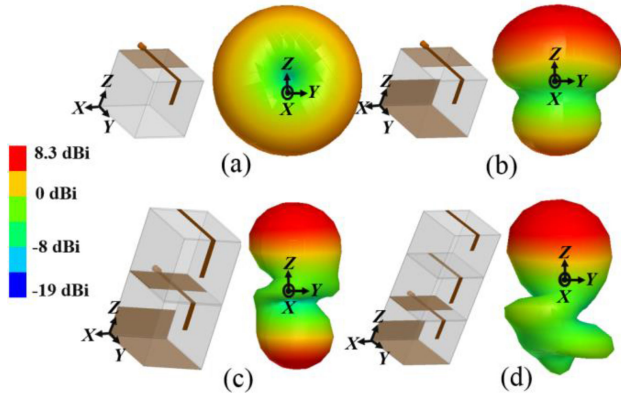

Fig. 4. Simulated 3-D radiation patterns for the antennas at each design step. (a) Driven element. (b) Driven element with reflector. (c) Driven element with reflector and one director. (d) Driven element with reflector and two directors.
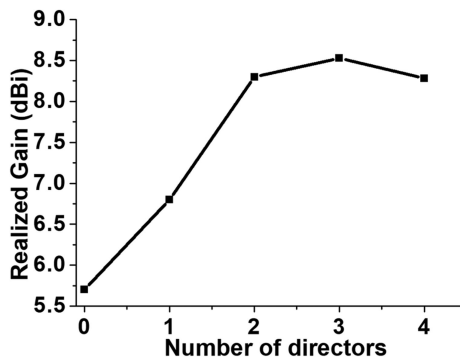

Fig. 5. Relationship between the peak gain and the number of directors.

the peak gain. As shown in Fig. 5, the peak gain is significantly increased up to two directors. However, the gain enchantment is not substantial with the subsequent addition of the third director, while the peak gain is slightly decreased after adding four directors.
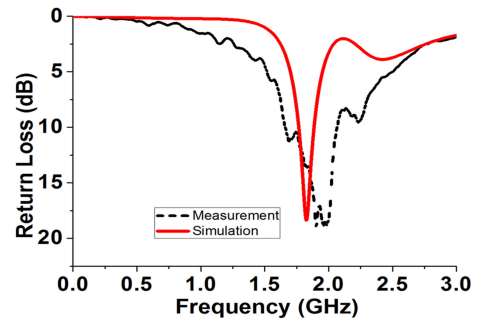

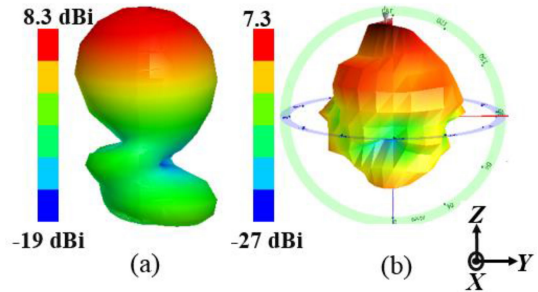Fig. 6. Simulated and measured return losses for the proposed antenna in the unfolded state.

Fig. 7. 3-D radiation patterns for the proposed origami antenna at 1.9 GHz. (a) Simulated. (b) Measured.

III. MEASUREMENT RESULTS

The designed antenna was constructed by joining three origami magic cubes as shown in Fig. 2, with the unfolded and folded states in Fig. 2(v) and (w), respectively. The *S*-parameters were measured in the unfolded state using an Anritsu vector network analyzer (MS2038C), and simulated and measured reflection coefficients are compared in Fig. 6.

The measured return loss >10 dB was obtained from 1.65 to 2.05 GHz, whereas the simulation return loss >10 dB was achieved from 1.76 to 1.9 GHz. The 3-D radiation pattern was measured at 1.9 GHz in an anechoic chamber, as shown in Fig. 7. The measured peak gain was found to be 7.3 dBi, whereas the simulated peak gain is 8.3 dBi. Thus, the measured impedance bandwidth was slightly wider than that of the simulated response, which is mostly due to the loss of the paper material. This lossy characteristic also slightly reduced the measured gain as compared to the simulated peak gain.

IV. CONCLUSION

We proposed a low-cost deployable quasi-Yagi monopole antenna using three origami magic spiral cubes. The L-shaped reflector and two directors increased peak gain from 1.9 to 7.3 dBi at 1.9 GHz. Thus, the L-shaped driven monopole, reflector, and director geometries have successfully maximized directivity in a limited cube size. The folded antenna is only 6% of the volume of the unfolded state, allowing easy transport and deployment, and the origami magic cube construction provides stable folding and unfolding. Since the origami magic spiral cubes are constructed from folded plain paper sheets, the proposed antenna provides very simple and fast fabrication. A radome can be employed to protect the proposed geometry from adverse environments for practical outdoor applications.

REFERENCES

[1] S.-J. Lee, W.-S. Yoon, and S.-M. Han, "Planar directional beam antenna design for beam switching system applications," *J. Electromagn. Eng. Sci.*, vol. 17, no. 1, pp. 14–19, 2017.

[2] P. Duangtang, P. Mesawad, and R. Wongsan, "Creating a gain enhancement technique for a conical horn antenna by adding a wire medium structure at the aperture," *J. Electromagn. Eng. Sci.*, vol. 16, no. 2, pp. 134–142, 2016.

[3] J. L. Silverberg *et al.*, "Using origami design principles to fold re-programmable mechanical metamaterials," *Science*, vol. 345, no. 6197, pp. 647–650, 2014.

[4] E. Hawkes *et al.*, "Programmable matter by folding," *Proc. Nat. Acad. Sci.*, vol. 107, no. 28, pp. 12441–12445, 2010.

[5] B. G. G. Chen *et al.*, "Topological mechanics of origami and kirigami," *Phys. Rev. Lett.*, vol. 116, no. 13, pp. 1–5, 2016.

[6] L. H. Dudte, E. Vouga, T. Tachi, and L. Mahadevan, "Programming curvature using origami tessellations," *Nat. Mater.*, vol. 15, no. 5, pp. 583–588, 2016.

[7] Z. Song *et al.*, "Origami lithium-ion batteries," *Nat. Commun.*, vol. 5, pp. 1–6, 2014.

[8] R. V. Martinez, C. R. Fish, X. Chen, and G. M. Whitesides, "Elastomeric origami: Programmable paper-elastomer composites as pneumatic actuators," *Adv. Funct. Mater.*, vol. 22, no. 7, pp. 1376–1384, 2012.

[9] J. P. Gardner *et al.*, "The James Webb space telescope," *Space Sci. Rev.*, vol. 123, no. 4, pp. 485–606, 2006.

[10] K. Kuribayashi *et al.*, "Self-deployable origami stent grafts as a biomedical application of Ni-rich TiNi shape memory alloy foil," *Mater. Sci. Eng., A*, vol. 419, no. 1/2, pp. 131–137, 2006.

[11] S. I. H. Shah, M. M. Tentzeris, and S. Lim, "Low-cost circularly polarized origami antenna," *IEEE Antennas Wireless Propag. Lett.*, vol. 16, pp. 2026–2029, 2017.

[12] X. Liu, S. Yao, B. S. Cook, M. M. Tentzeris, and S. V. Georgakopoulos, "An origami reconfigurable axial-mode bifilar helical antenna," *IEEE Trans. Antennas Propag.*, vol. 63, no. 12, pp. 5897–5903, Dec. 2015.

[13] X. Liu, S. Yao, P. Gonzalez, and S. V. Georgakopoulos, "A novel ultra-wideband origami reconfigurable quasi-taper helical antenna," in *Proc. Int. Symp. IEEE Antennas Propag. Soc.*, 2016, pp. 839–840,

[14] X. Liu, S. Yao, S. V. Georgakopoulos, B. S. Cook, and M. M. Tentzeris, "Reconfigurable helical antenna based on an origami structure for wireless communication system," in *Proc. Int. Symp. IEEE MTT-S Microw.*, 2014, vol. 1, pp. 2–5.

[15] S. Shah and S. Lim, "A dual band frequency reconfigurable origami magic cube antenna for wireless sensor network applications," *Sensors*, vol. 17, no. 11, 2017, Art. no. 2675.

[16] X. Liu, S. V Georgakopoulos, and S. Rao, "A design of an origami reconfigurable QHA with a foldable reflector [antenna applications corner]," *IEEE Antennas Propag. Mag.*, vol. 59, no. 4, pp. 78–105, Aug. 2017.

[17] S. Yao, X. Liu, and S. V. Georgakopoulos, "Morphing origami conical spiral antenna based on the Nojima wrap," *IEEE Trans. Antennas Propag.*, vol. 65, no. 5, pp. 2222–2232, May 2017.

[18] S. I. H. Shah and S. Lim, "Transformation from a single antenna to a series array using push/pull origami," *Sensors*, vol. 17, no. 9, 2017, Art. no. 1968.

[19] S. Yao and S. V. Georgakopoulos, "Origami segmented helical antenna with switchable sense of polarization," *IEEE Access*, vol. 6, pp. 4528–4536, 2017.

[20] X. Liu, S. Yao, and S. V. Georgakopoulos, "Reconfigurable origami equiangular conical spiral antenna," in *Proc. Int. Symp. IEEE Antennas Propag. Soc.*, 2015, pp. 2263–2264,

[21] S. I. H. Shah, D. Lee, M. Tentzeris, and S. Lim, "A novel high-gain tetrahedron origami antenna," *IEEE Antennas Wireless Propag. Lett.*, vol. 16, pp. 848–851, 2016.